miR-769-5p is associated with prostate cancer recurrence and modulates proliferation and apoptosis of cancer cells

DANIEL LEE

Medical Oncology Service and The Center for Cancer Research, National Cancer Institute, National Institutes of Health, Bethesda, MD 20892, USA

Received May 15, 2020; Accepted December 15, 2020

DOI: 10.3892/etm.2021.9766

Abstract. MicroRNAs (miRs) are relevant in biological processes, including human prostate cancer. In the present study, the role of miR-769-5p and its targets in prostate cancer were explored. Publicly available data on expression of genes, miRs and disease-free survival of patients with prostate cancer were analyzed along with RNAseq of transfected cell lines. miR-769-5p expression was inversely associated with patient survival and *in vitro* assays indicated that its inhibition reduced the proliferation and increased apoptosis of prostate cancer cells. miR-769-5p was revealed to target Rho GTPase activating protein 10 (ARHGAP10) and increased expression of ARHGAP10 in tumors was determined to be associated with a favorable prognosis regarding disease-free survival. Of note, ARHGAP10 is a purported tumor suppressor in ovarian cancer, where it inhibits cell division cycle 42 (CDC42) activity and increases apoptosis. Similar effects were observed in prostate cancer cells, where miR-769-5p inhibition increased ARHGAP10 and led to reduced CDC42 activity. Furthermore, miR-769-5p inhibition increased apoptosis, which was partly reversed by additional knockdown of ARHGAP10. These results suggested that miR-769-5p is an oncogene targeting ARHGAP10, which in turn is a candidate tumor suppressor in prostate cancer.

Introduction

Since the initial report in *C. elegans* (1), microRNAs (miRNAs/miRs) and their supposed roles have been described in different organisms and human diseases, including cancers. miRs have been reported to be involved in cancer progression, such as miR-1 and miR-106b-25 in prostate carcinogenesis (2-4).

In order to identify additional miRs relevant to disease progression, research efforts have concentrated on the miRs associated with survival. Utilizing a publicly available database of miRs in prostate cancer (5), miR-769-5p was identified and its expression predicted disease-free survival of patients with prostate cancer. There have been certain reports on miR-769-5p in cancer. For instance, miR-769-5p was indicated to be a prognostic biomarker for survival in pancreatic cancer (6), and it was highly expressed in Merkel cell carcinoma with positivity for Merkel cell polyomavirus vs. those that were negative (7). It was also reported to be a prognostic biomarker in non-small cell lung cancer (NSCLC) (8) and inhibited NSCLC tumorigenesis *in vitro* and *in vivo* (9). All of these studies suggested a potential function of miR-769-5p as an oncogene, but its role in prostate cancer has not been previously reported. Of note, one of its potential targets is Rho GTPase activating protein 10 (ARHGAP10), a putative tumor suppressor in ovarian cancer (10). In addition, ARHGAP10 expression has been reported to be positively associated with the survival of patients with prostate cancer (11); thus, it appeared worthwhile to investigate the relationship between miR-769-5p and ARHGAP10 within the context of prostate cancer.

In the present study, it was hypothesized that miR-769-5p acts as an oncogene by targeting ARHGAP10 to achieve its degradation. Inhibition of miR-769-5p affected the proliferation and apoptosis of prostate cancer cells, the latter of which was partially counteracted by knockdown of ARHGAP10, likely in concert with cell division cycle (CDC)42.

Materials and methods

Cell lines. The normal cell line RWPE-1 and the cancerous cell lines 22Rv1, LNCaP, MDA-PCa-2b, DU145, PC-3 and HEK-293 were obtained from the American Type Culture Collection. The following media were used for the cells: RWPE-1, Keratinocyte serum free medium (K-SFM) + EGF + bovine pituitary extract (BPE) (Gibco cat. no. 17005-042); 22Rv1, RPMI (Gibco; Thermo Fisher Scientific, Inc.; cat. no. 11875-093) + 10% FBS (R&D systems; cat. no. S12450); LNCaP, RPMI (Gibco;

Correspondence to: Dr Daniel Lee, Medical Oncology Service and The Center for Cancer Research, National Cancer Institute, National Institutes of Health, 10 Center Drive, B2L312, Bethesda, MD 20892, USA
E-mail: beaver9701@gmail.com

Abbreviations: miR, microRNA; NSCLC, non-small cell lung cancer; TCGA, The Cancer Genome Atlas; UTR, untranslated region

Key words: prostate cancer recurrence, miR-769-5p, Rho GTPase activating protein 10

Thermo Fisher Scientific, Inc.; cat. no. 11875-093) + 10% FBS (R&D Systems; cat. no. S12450); MDA-PCa-2b, F12K (ATCC; cat. no. 30-2004) + 20% FBS (R&D systems; cat. no. S12450) + 25 ng/ml cholera toxin (Sigma-Aldrich; Merck KGaA; cat. no. C8052) + 10 ng/ml mouse epidermal growth factor (Corning, Inc.; cat. no. 354010) + 0.005 mM phosphoethanolamine (Sigma-Aldrich; Merck KGaA; cat. no. P0503) + 100 pg/ml hydrocortisone (Sigma-Aldrich; Merck KGaA; cat. no. H0135) + 45 nM sodium selenite (Sigma-Aldrich; Merck KGaA; cat. no. 9133) + 0.005 mg/ml human recombinant insulin (Thermo Fisher Scientific, Inc.; cat. no. 12585-014); DU145, MEM (Gibco; Thermo Fisher Scientific, Inc.; cat. no. 11095-080) + 10% FBS (R&D systems, Inc.; cat. no. S12450); PC-3, F12 (Gibco; Thermo Fisher Scientific, Inc.; cat. no. 11765-054) + 10% FBS (R&D systems, Inc.; cat. no. S12450); HEK-293, MEM (Gibco; Thermo Fisher Scientific, Inc.; cat. no. 11095-080) + 10% FBS (R&D Systems, Inc.; cat. no. S12450). All cells were cultured at 37˚C in a humidified atmosphere containing 5% CO_2. A short tandem repeat analysis with GenePrint10 was performed for regular authentication and the cells were regularly tested for mycoplasma contamination.

RNA extraction and reverse transcription-quantitative PCR and (RT-qPCR). Total RNA was isolated using TRIzol (Thermo Fisher Scientific, Inc.; cat. no. 15596026) according to the manufacturer's protocol. For RT-qPCR of miRNA, 10 ng total RNA was reverse transcribed using the TaqMan MicroRNA Reverse Transcription kit (Thermo Fisher Scientific, Inc.; cat. no. 4366596) according to the manufacturer's protocol. The expression levels of miR-769-5p were assessed in triplicate using TaqMan probes for miR-769-5p (Thermo Fisher Scientific, Inc.; cat. no. 4427975; assay ID 001998) and the internal standard reference U6 small nuclear RNA (Thermo Fisher Scientific, Inc.; cat. no. 4427975; assay ID 001973) with TaqMan Universal Master Mix II (not containing uracil-DNA glycosylase; Thermo Fisher Scientific, Inc.; cat. no. 4440041).

For RT-qPCR analysis of mRNAs, 1 μg total RNA was reverse transcribed using the High-Capacity cDNA Reverse Transcription Kit with RNase Inhibitor (Thermo Fisher Scientific, Inc.; cat. no. 4374967) according to the manufacturer's instructions. Expression levels of genes were assessed in triplicate using TaqMan probes for 1-acyl-sn-glycerol-3-phosphate acyltransferase α (Thermo Fisher Scientific, Inc.; cat. no. 4331182; assay ID Hs00965850_g1), Kremen protein 1 (Thermo Fisher Scientific, Inc.; cat. no. 4331182; assay ID Hs00230750_m1), cyclin-D1-binding protein 1 (Thermo Fisher Scientific, Inc.; cat. no. 4351372; assay ID Hs01050839_m1), ARHGAP10 (Rho GTPase-activating protein 10; Thermo Fisher Scientific, Inc.; cat. no. 4331182; assay ID Hs00226305_m1), FHL3 (four and a half LIM domains protein 3; Thermo Fisher Scientific, Inc.; cat. no. 4331182; assay ID Hs00916408_g1), KCTD11 (Potassium Channel Tetramerisation Domain Containing 11; Thermo Fisher Scientific, Inc.; cat. no. 4331182; assay ID Hs00922550_s1) and the internal standard reference 18s ribosomal (r)RNA (Thermo Fisher Scientific, Inc.; cat. no. 4331182; assay ID Hs99999901_s1) with TaqMan Gene Expression Master Mix (Thermo Fisher Scientific, Inc.; cat. no. 4369016).

Owing to the high abundance of 18s rRNA, total RNA was diluted 1:100 for the 18s rRNA assay yielding average C_qs of 13-20. Assays were run on a MicroAmp Optical 384-Well Reaction Plate with Barcode (cat. no. 4343814). The following thermocycling conditions were used: 1-2 min at 50˚C, 2-10 min at 95˚C, 3-15 sec at 95˚C and 4-60 sec at 60˚C, repeated x40. Results were then analyzed using 7900HT Fast Real-Time PCR System with a 384-well block module (Thermo Fisher Scientific, Inc.; cat. no. 4329001). To calculate normalized expression levels, the comparative C_q method was used and fold changes for miR-769-5p or each gene were obtained from the $2^{\Delta\Delta Cq}$ values (12).

Cell proliferation. Human prostate cells were seeded at $2x10^5$ cells/well in 6-well plates and transfected using one of two different protocols: i) At 24 h after seeding, the cells were transfected with 30 nM mirVana miRNA inhibitor, negative control #1 (Thermo Fisher Scientific, Inc.; cat. no. 4464076) or mirVana miR-769-5p inhibitor (Thermo Fisher Scientific, Inc.; cat. no. 4464084, assay ID MH11974) using Lipofectamine RNAiMAX (Thermo Fisher Scientific, Inc.; cat. no. 13778150). By using RT-qPCR, a 40-50% reduction of miR-769-5p was verified, which was induced by the inhibitor relative to the negative control. ii) At 24 h after seeding, the cells were transfected with one of the following: a) 30 nM each of mirVana miRNA inhibitor, negative control #1 (Thermo Fisher Scientific, Inc.; cat. no. 4464076) and Silencer Select negative control #1 siRNA (Thermo Fisher Scientific, Inc.; cat. no. 4390843); b) 30 nM each of mirVana miR-769-5p inhibitor (Thermo Fisher Scientific, Inc.; cat. no. 4464084, assay ID MH11974) and Silencer Select negative control #1 siRNA (Thermo Fisher Scientific, Inc.; cat. no. 4390843); or c) 30 nM each of mirVana miR-769-5p inhibitor (Thermo Fisher Scientific, Inc.; cat. no. 4464084, assay ID MH11974) and ARHGAP10 Silencer Select small interfering (si)RNAs (Thermo Fisher Scientific, Inc.; cat. no. 4392420, IDs s36028 and s36029) using Lipofectamine RNAiMAX (Thermo Fisher Scientific, Inc.; cat. no. 13778150). Downregulation of miR-769-5p and upregulation of ARHGAP10 in response to mirVana miRNA inhibitor were verified by RT-qPCR. Furthermore, downregulation of ARHGAP10 in response to ARHGAP10 siRNAs was verified.

After 48 h of transfection, 4 columns of wells were seeded in a 96-well plate with each of the following for the 2 transfection groups: i) 100 μl of media/well with no cells, $1x10^3$ negative control-transfected cells/well or $1x10^3$ miR-769-5p inhibitor-transfected cells/well; ii) 100 μl of media/well with no cells, $1x10^3$ negative control miR- and siRNA control-transfected cells/well, $1x10^3$ miR-769-5p inhibitor- and siRNA control-transfected cells/well or $1x10^3$ miR-769-5p inhibitor- and ARHGAP10 siRNA-transfected cells/well. Each column of wells represented 8 replicates for a specific time-point (days 0, 1, 3 or 5).

Cell viability was measured on days 0, 1, 3 and5 using alamarBlue Cell Viability Reagent (Thermo Fisher Scientific, Inc.; cat. no. DAL1025) with a FLUOstar Omega microplate reader from BMG Labtech, using fluorescence (excitation, 544 nm/emission, 590 nm). Background fluorescence values of media-only wells were subtracted from the values of wells with treated cells. The subtracted fluorescence

values of the 8 replicate wells from on day 5 were compared as follows for the 2 transfections: i) Negative control vs. miR-769-5p inhibitor-transfected cells. ii) miR control and siRNA control vs. miR-769-5p inhibitor and siRNA control. miR control and siRNA control vs. miR-769-5p inhibitor and ARHGAP10 siRNAs. The experiment was performed as three independent replicates for both transfection conditions.

Apoptosis. The seeding and transfection conditions were as follows: i) Cells were seeded at $1.6x10^6$ cells/well in T25 flasks (n=9). At 24 h after seeding, the cells were transfected with 30 nM mirVana miRNA inhibitor, negative control #1 (Thermo Fisher Scientific, Inc.; cat. no. 4464076) or mirVana miR-769-5p inhibitor (Thermo Fisher Scientific, Inc.; cat. no. 4464084, assay ID MH11974) using Lipofectamine RNAiMAX (Thermo Fisher Scientific, Inc.; cat. no. 13778150). A 40-50% reduction of miR-769-5p induced by the inhibitor relative to the negative control was verified by RT-qPCR. ii) PC-3 cells were seeded at $1.6x10^6$ cells/well in T25 flasks (n=7). At 24 h after seeding, the cells were transfected with one of the following: i) 30 nM each of mirVana miRNA inhibitor, negative control #1 (cat. no. 4464076) and Silencer Select negative control #1 siRNA (cat. no. 4390843); ii) 30 nM each of mirVana miR-769-5p inhibitor (cat. no. 4464084, assay ID MH11974) and Silencer Select negative control #1 siRNA (cat. no. 4390843); or iii) 30 nM each of mirVana miR-769-5p inhibitor (cat. no. 4464084, assay ID MH11974) and ARHGAP10 Silencer Select siRNAs (cat. no. 4392420, IDs s36028 and s36029) using Lipofectamine RNAiMAX (cat. no. 13778150), all from Thermo Fisher Scientific, Inc. Downregulation of miR-769-5p and upregulation of ARHGAP10 in response to mirVana miRNA inhibitor were verified by RT-qPCR. Furthermore, downregulation of ARHGAP10 in response to ARHGAP10 siRNAs was verified.

At 48 h after transfections, $1.2x10^6$ cell pellets from each treatment group were harvested and frozen at -80˚C. Caspase-3 levels, an indicator of apoptosis, were measured in cell pellets using the EnzChek Caspase-3 Assay Kit #2 (Thermo Fisher Scientific, Inc.; cat. no. E13184). and a FLUOstar Omega microplate reader from BMG Labtech, using fluorescence (excitation, 485 nm/emission, 520 nm). The caspase-3 levels were compared as follows for the 2 transfections: i) Negative control vs. miR-769-5p inhibitor-transfected cells. ii) miR control and siRNA control vs. miR-769-5p inhibitor and siRNA control. miR control and siRNA control vs. miR-769-5p inhibitor and ARHGAP10 siRNAs.

Migration and invasion assays. DU145 or PC-3 cells were seeded at $2x10^5$ cells/well in 6-well plates. At 24 h after seeding, the cells were transfected with 30 nM mirVana miRNA inhibitor, negative control #1 (Thermo Fisher Scientific, Inc.; cat. no. 4464076) or mirVana miR-769-5p inhibitor (Thermo Fisher Scientific, Inc.; cat. no. 4464084, assay ID MH11974) using Lipofectamine RNAiMAX (Thermo Fisher Scientific, Inc.; cat. no. 13778150). A 40-50% reduction of miR-769-5p induced by the inhibitor relative to the negative control was verified (Fig SI).

Migration assay. After 48 h of transfection, $3x10^4$ DU145 cells were seeded for each treatment condition in replicate wells in the upper chamber of a cell invasion and migration (CIM) plate 16 (ACEA Biosciences; cat. no. 05665817001), whose bottom chamber contained media with 10% FBS (R&D systems, Inc.; cat. no. S12450) as an attractant. The chambers of a CIM plate 16 were assembled and loaded onto xCELLigence RTCA Systems (ACEA Biosciences; cat. no. 00380601050). The xCELLigence machinery quantified cell movements from the upper to the bottom chambers in 15-min intervals for 48 h. The experiment was performed as three independent replicates.

Invasion assay. The steps described for the migration assay were reperformed with PC-3 cells with two additional steps: Prior to seeding of the cells onto the plate, the wells in the upper chamber of the CIM plate 16 (ACEA Biosciences; cat. no. 05665817001) were coated with 5% Matrigel Matrix (BD Biosciences; cat. no. 356234), and the upper chamber was placed in a 37˚C incubator for 4 h for the Matrigel to solidify.

RNA sequencing (RNAseq) and strategy to obtain gene targets of miR-769-5p. DU145 and PC-3 cells were transfected with 100 nM of mirVana miRNA mimics, negative control #1 (Thermo Fisher Scientific, Inc.; cat. no. 4464058) or miR-769-5p mimics (Thermo Fisher Scientific, Inc.; cat. no. 4464066, assay ID MC11974) in quadruplicates and submitted to RNAseq, whose workflow was as follows: The Sequencing Facility was at Leidos Biomedical Research, Inc., Frederick National Laboratory for Cancer Research performed RNA sequencing. For library preparation, the TruSeq V3 chemistry kit from Illumina, Inc. was used with 500 ng total RNA. The Illumina HiSeq 2000 system was utilized for sequencing. For each sample, ~50 million paired-end reads with a length of 101 bp were generated. Trimmomatic software version 0.36 (usadellab.org) was used for trimming reads for both adapters and low-quality bases and the Tophat software version 2.1.1 (http://ccb.jhu.edu/software/tophat/index.shtml) was used for aligning the trimmed reads with the reference human hg19 genome and gene annotation from the Ensembl database (http://grch37.ensembl.org/index.html). Picard software version 2.0.1 (https://broadinstitute.github.io/picard/) was used for calculating RNA mapping statistics and the average uniquely aligned reads were ~90% for all samples. The RNA-seq workflow module in Partek Genomics Suite 6.6 (Partek, Inc.) and the R/Bioconductor package DESeq2 version 3.12 (https://bioconductor.org/packages/release/bioc/html/DESeq2.html) were used to identify differentially expressed genes with a false discovery rate of <5% and a fold change (≤-1.5) as cut-offs. Partek was utilized to perform an analysis based on reads per kilobase per million mapped reads and it allowed the gene counts to be fitted to a negative binomial generalized linear model with DESeq2.

Strategy. The TargetScan database (http://www.targetscan.org) was utilized to generate a list of predicted gene targets of miR-769-5p. In order to generate an overlap between TargetScan-predicted targets and the RNAseq-downregulated transcripts in miR-769-5p mimics-transfected DU145 or PC-3 cells [cut-off: P<0.01 and ≤-1.5 fold expression change (5)], the Oliveros, J.C. (2007-2015) Venny software (http://bioinfogp.

cnb.csic.es/tools/venny/index.html), an interactive tool for comparing lists using Venn diagrams, was applied.

In order to reduce the list of genes from the overlap (322 candidate genes for DU145 and 280 for PC-3), the expression of genes in prostate tumor vs. non-cancerous tissues from 8 cohorts [Grasso *et al* (13), Lapointe *et al* (14), Singh *et al* (15), Taylor *et al* (5), The Cancer Genome Atlas (TCGA) (16), Tomlins *et al* (17), Wallace *et al* (18) and Yu *et al* (19)] was obtained from Oncomine (http://www.oncomine.org, December 2016, Thermo Fisher Scientific, Inc.). The gene lists for DU145 and PC-3 were compared with the gene lists from these 8 cohorts. Entries with an overlap with genes that had a higher expression in normal tissue vs. tumors in ≥2 cohorts were selected and they were searched in PubMed. Subsequently, the list of potential tumor suppressors targeted by miR-769-5p was further reduced.

Luciferase reporter assay. The TargetScan database (http://www.targetscan.org) was utilized to locate the putative binding sites of miR-769-5p in the 3'-untranslated region (3'-UTR) of ARHGAP10 and to generate 4 constructs, 1 wild-type (WT) and 3 mutants (MUT). The reporter construct, pLenti-UTR-Luc, contains a cytomegalovirus (CMV) promoter followed by luciferase from *Photinus pyralis*, and it was digested with *Eco*RI and *Xho*I. The 3'-UTR sequences of ARHGAP10 WT, ARHGAP10 MUT1, ARHGAP10 MUT2 and ARHGAP10 MUT1+2 were amplified by PCR from human genomic DNA (isolated from HEK-293 using DNAzol, Thermo Fisher Scientific, Inc. cat. no. 10503027, according to the manufacturer's instructions) plus complementary DNA as follows: PCR was used to amplify the WT sequence with primers at both ends. The MUT1, MUT2 and MUT1+2 were amplified using outer primers together with internal primers that carried the mutation. A Ligation-Free Cloning kit (cat. no. E001) from ABM was used to assemble the 2 PCR amplicons into 1 mutant 3'-UTR, feasible due to the overlapping sequences of the 2 internal primers. Each 3'-UTR was inserted into the reporter construct using the Ligation-Free Cloning kit. The sequences of the 4 WT and MUT constructs were verified using Macrogen (https://dna.macrogen.com/main.do#) (Table SI).

A total of $7x10^4$ DU145 cells per well were seeded in 24-well plates and co-transfected with 100 nM mirVana miRNA mimics, negative control #1 (Thermo Fisher Scientific, Inc.; cat.no.4464058) or miR-769-5p mimics (Thermo Fisher Scientific, Inc.; cat. no. 4464066, assay ID MC11974), 100 ng of luciferase reporter pLenti-UTR-Luc ARHGAP10 WT, pLenti-UTR-Luc ARHGAP10 MUT1, pLenti-UTR-Luc ARHGAP10 MUT2 or pLenti-UTR-Luc ARHGAP10 MUT1+2 and 4 ng of pRL-CMV *Renilla* luciferase reporter (Promega; cat. no. E2261) using TransIT-X2 (Mirus; cat. no. 6004). Subsequently, the cells were cultured for 48 h and washed with PBS. Using a Luc-Pair Duo-Luciferase HS Assay kit (GeneCopoeia; cat. no. LF004), the cells were lysed, the lysates were loaded onto white 96 wells in quadruplicates and their luciferase/*Renilla* ratios were measured using a FLUOstar Omega microplate reader (BMG Labtech). The experiment was performed, n=5.

CDC42 activity measurement. DU145 cells were seeded at $2x10^5$ cells/well in 6-well plates (n=6 experiments). At 24 h after seeding, the cells were transfected with one of the following: i) 30 nM each of mirVana miRNA inhibitor, negative control #1 (Thermo Fisher Scientific, Inc.; cat. no. 4464076) and Silencer Select negative control #1 siRNA (Thermo Fisher Scientific, Inc.; cat. no. 4390843); ii) 30 nM each of mirVana miR-769-5p inhibitor (Thermo Fisher Scientific, Inc.; cat. no. 4464084; assay ID MH11974) and Silencer Select negative control #1 siRNA (Thermo Fisher Scientific, Inc.; cat. no. 4390843); or iii) 30 nM each of mirVana miR-769-5p inhibitor (Thermo Fisher Scientific, Inc.; cat. no. 4464084; assay ID MH11974) and ARHGAP10 Silencer Select siRNAs (Thermo Fisher Scientific, Inc.; cat. no. 4392420; assay IDs s36028 and s36029) using Lipofectamine RNAiMAX (Thermo Fisher Scientific, Inc.; cat. no. 13778150). Downregulation of miR-769-5p and upregulation of ARHGAP10 in response to mirVana miRNA inhibitor transfection were verified. Furthermore, downregulation of ARHGAP10 in response to ARHGAP10 siRNAs was verified.

At 48 h after transfection, cell lysates were harvested on ice as per the instructions for the CDC42 G-LISA Activation Assay (Cytoskeleton, Inc.; cat. no. BK127). Protein concentrations were measured according to the manufacturer's instructions using Precision Red™ Advanced Protein Assay Reagent, absorbance at 600 nm. The equation used is as follows: $C=A/\varepsilon l$; where C = protein concentration (mg/ml), A = absorbance, l = pathlength (cm) and ε = extinction coefficient [$(mg/ml)^{-1}$ cm^{-1}]. The samples were normalized accordingly. CDC42 activity was measured according to the manufacturer's protocol. CDC42 activity was compared as follows: miR control and siRNA control vs. miR-769-5p inhibitor and siRNA control; and miR control and siRNA control vs. miR-769-5p inhibitor and ARHGAP10 siRNAs.

Statistical analysis and usage of public databases. A two-sided, unpaired t-test with Welch's correction was used to assess the endpoints, including differences in miRNA expression, proliferation, apoptosis and results of the luciferase assays. Welch's ANOVA with Dunnett's test was used for comparing >2 groups for miRNA and mRNA expression, CDC42 activity and apoptosis. Kaplan-Meier analysis was utilized to compare the differences in disease-free survival between groups of patients divided by miR-769-5p and/or ARHGAP10 expression.

TCGA data on prostate cancer were downloaded from the cBio Cancer Genomics Portal (http://cbio.mskcc.org/cancergenomics/prostate/data/) to obtain the expression of miR-769-5p and ARHGAP10 in patients. The data from Taylor *et al* (5) were downloaded from the National Center for Biotechnology Information (NCBI, https://www.ncbi.nlm.nih.gov/) to obtain miR-769-5p expression, ARHGAP10 expression and disease-free survival data of patients according to the expression of miR-769-5p and ARHGAP10. Recurrence-associated transcripts from Taylor *et al* (5) were derived utilizing Partek Genomics Suite 6.6 from Partek using Cox proportional hazards regression. The Spearman correlation between ARHGAP10 and miR-769-5p expression in tumor samples from Taylor *et al* (5) was determined.

For t-tests, Welch's ANOVA with Dunnett's test, Kaplan-Meier and Spearman analyses, GraphPad Prism 7.0

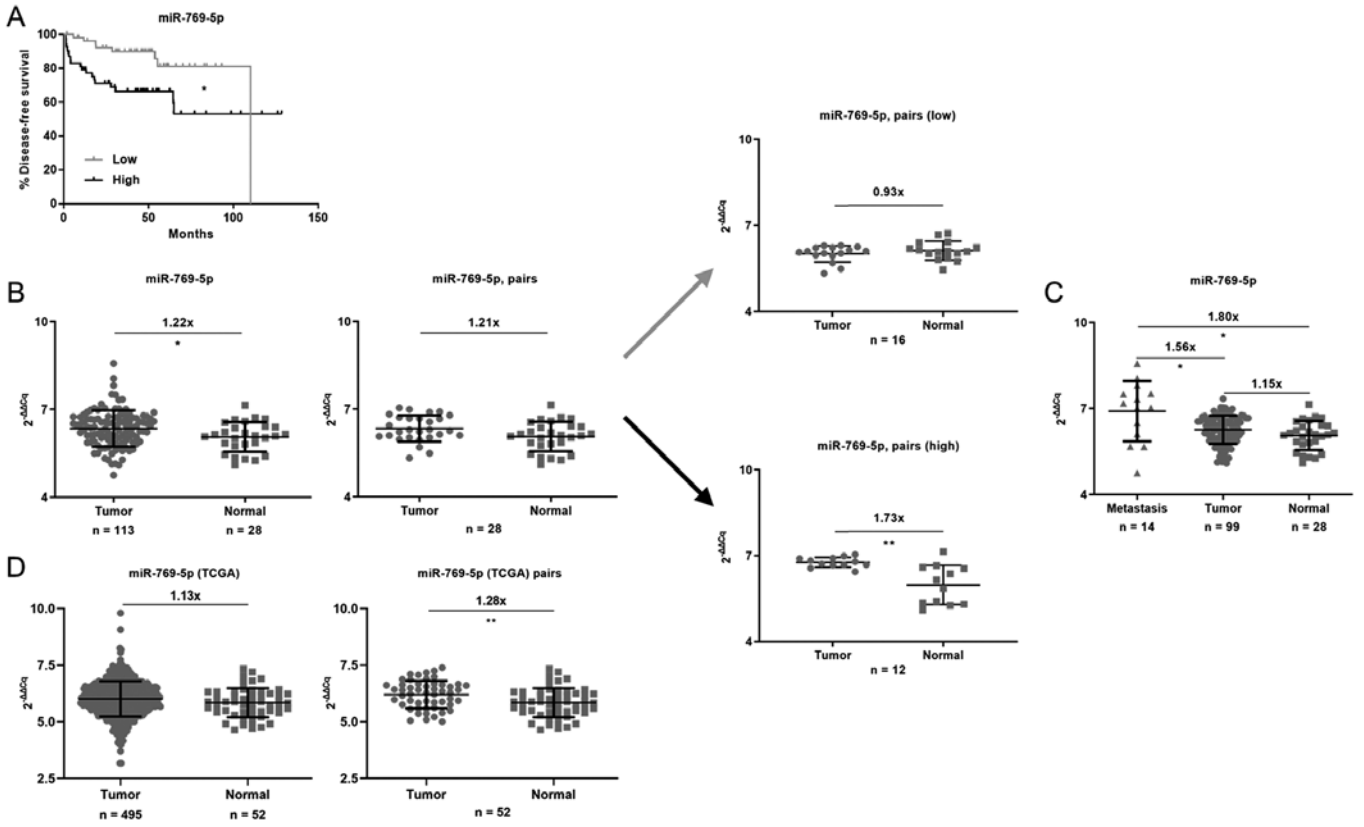

Figure 1. Analyses of miR-769-5p expression and its impact on survival. (A) Kaplan-Meier survival analysis suggested that miR-769-5p expression was inversely associated with disease-free survival. Data were extracted from Taylor *et al* (5) *P<0.05 according to the log-rank test with n=107. The patients were stratified into groups of high and low expression of miR-769-5p by assigning the bottom 50% (n=54) to the 'Low' and the top 50% (n=53) to the 'High' group according to their rank of miR-769-5p expression. Low: 46 censored, 8 events. High: 34 censored, 19 events. (B) miR-769-5p expression was elevated in tumor vs. normal tissues among all cases. In an analysis of matched pairs (n=28), the difference in miR-769-5p expression was not significant. However, after dividing the patients into groups with low (gray arrow) or high expression (black arrow) in the tumors, the difference in miR-769-5p expression between tumor and adjacent non-cancerous tissue was significant in the latter group. (C) When subdivided into 3 groups, miR-769-5p expression was the highest in metastasis, followed by tumor and then normal tissues. For B and C, normalized miR-769-5p expression data were extracted from Taylor *et al* (5) and fold differences were calculated using $2^{-\Delta\Delta Cq}$. (D) Analysis of all TCGA samples indicated that the difference in miR-769-5p expression between tumor and normal tissue did not reach statistical significance, but in matched pairs (n=52), miR-769-5p expression was significantly elevated in tumor vs. normal tissues. Normalized miR-769-5p expression data were extracted from TCGA and fold differences were calculated using $2^{-\Delta\Delta Cq}$. *P<0.05, **P<0.01 according to an unpaired t-test with Welch's correction or Welch's ANOVA with Dunnett's test in C. miR, microRNA; TCGA, The Cancer Genome Atlas.

(GraphPad Software, Inc.) was utilized. P<0.05 was considered to indicate statistical significance.

Results

Expression of miR-769-5p is inversely associated with disease-free survival and upregulated in human prostate tumors. Combination analysis of the publicly available data set (5) and utilization of the strategy (3) to dichotomize miRs into low or high expression groups based on their median values indicated that patients with high expression of miR-769-5p had significantly decreased disease-free survival compared with that of patients with low expression (Fig. 1A). Furthermore, the expression of miR-769-5p in tumor tissues was significantly higher compared with that in non-cancerous tissues in the complete dataset (Fig. 1B). While this difference did not reach statistical significance when focusing on only the matching pairs (n=28), a stratified analysis into high- and low-expressing tumors using the median miR-769-5p value as the cutoff revealed a prevalent upregulation of this miR in the subset of prostate tumors with high expression of miR-769-5p. In addition, miR-769-5p was significantly upregulated in metastases when compared to primary tumors and the non-cancerous tissues in the dataset (Fig. 1C). This phenomenon of higher expression of miR-769-5p in tumor compared to non-cancerous tissues was also observed in the TCGA dataset matching pairs (Fig. 1D). Taken together, the survival and expression data pointed towards miR-769-5p being a candidate oncogene.

Identification of protein-coding genes that are candidate targets of miR-769-5p. miR-769-5p expression was assessed in six human prostate cell lines by using RT-qPCR (Fig. 2A) and a trend toward a higher expression in the cancer cell lines was noted, specifically those derived from metastases compared to the non-tumorigenic RWPE1 and tumorigenic 22Rv1 cells (Fig. 2B). Therefore, it was reasoned that miR-769-5p may be most relevant in the metastatic cell lines and the two metastatic cell lines DU145 and PC-3 were used for the subsequent experiments.

miR-769-5p mimics were transfected into DU145 and PC-3 cells, followed by RNAseq and TargetScan analyses.

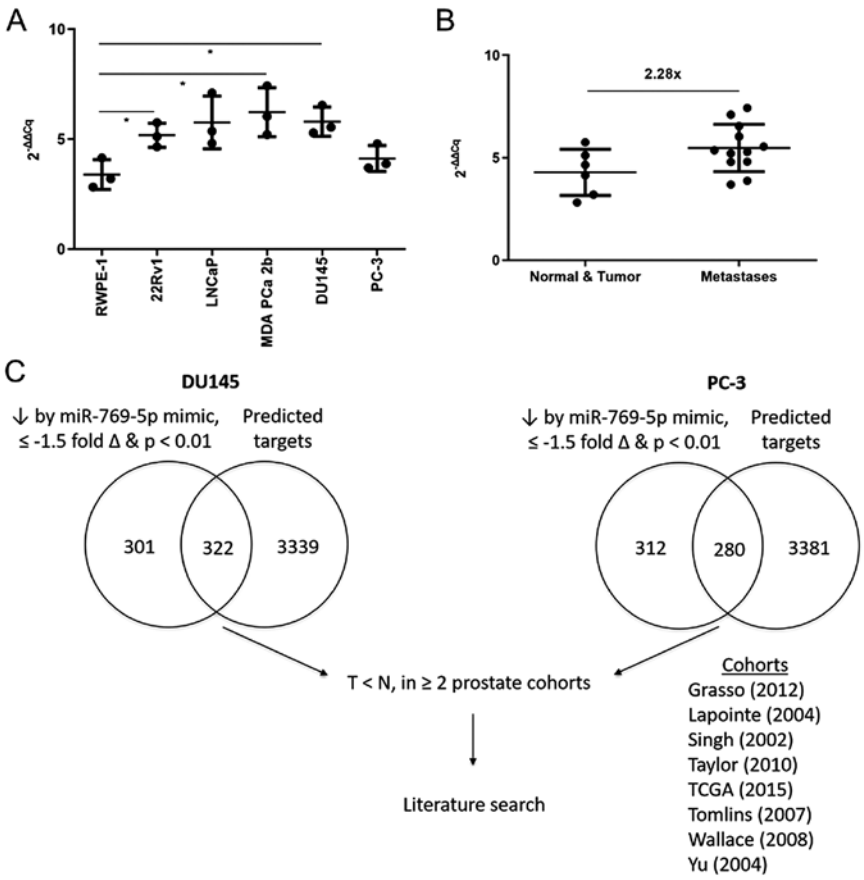

Figure 2. miR-769-5p expression in prostate cancer cells and scheme for identifying tumor suppressors targeted by the miR. (A) miR-769-5p expression in the six human prostate cell lines as assessed by quantitative PCR. (B) miR-769-5p expression in cell lines grouped by origin; comparison of 2 cell lines from normal and primary tumors (RWPE-1 and 22Rv1) vs. 4 cell lines from metastases (LNCaP, MDA PCa 2b, DU145 and PC-3). miR-769-5p expression fold differences between the 2 groups derived from the average miR expression in the 2 groups and calculated using the $2^{-\Delta\Delta Cq}$ method. Values are expressed as the mean ± standard deviation (n=3). *P<0.05 according to Welch's ANOVA with Dunnett's test in A and an unpaired t-test with Welch's correction in B. (C) The strengths of RNA sequencing, TargetScan, Oncomine cohorts and literature search were combined to identify potential tumor suppressors targeted by miR-769-5p. The 322 (DU145) and 280 (PC-3) candidate genes that overlapped with predicted TargetScan targets were compared to the genes differentially expressed in the 8 prostate cancer cohorts. The genes with a higher expression in normal tissue vs. tumor tissues in ≥2 cohorts were selected and searched using PubMed. miR, microRNA; TCGA, The Cancer Genome Atlas.

TargetScan is a bioinformatics tool for miR research that may be used to select candidate target genes of miRNAs relevant in carcinogenesis. Protein-coding genes that were predicted to be targets of miR-769-5p according to TargetScan were focused on, and they were required to exhibit significant downregulation 24 h after transfection of the miR mimics.

Subsequently, the downregulated genes in the DU145 (n=322) and PC-3 (n=280) cell lines from the overlap with TargetScan predictions (Fig. 2C and Table I) were compared against a list of candidate tumor suppressors (decreased expression in tumors compared with normal tissue in two Oncomine datasets) and a literature search was performed, focusing on potential tumor suppressors yet to be extensively reported. The aim was to combine the powers of RNAseq, TargetScan, Oncomine and literature searches to select tumor suppressors targeted by miR-769-5p. This approach yielded several candidates (Table SII) and the top six are presented in Fig. 3.

ARHGAP10 is a candidate target of miR-769-5p. Among the six candidates, only ARHGAP10, FHL3 and KCTD11 had the expected increase in expression upon treatment with a miR-769-5p inhibitor and decrease in expression following transfection of miR-769-5p mimics. ARHGAP10 expression had the largest fold change and the strongest association with the experimental miR-769-5p status. ARHGAP10 has been reported to be downregulated in ovarian cancer (10), having a tumor suppressor role. In addition, it is associated with a favorable prognosis for patients with prostate cancer (11). Therefore, subsequent experiments aimed to clarify the relationship between miR-769-5p and the candidate tumor suppressor ARHGAP10 in prostate cancer.

Moving forward, ARHGAP10 was indicated to be both a predicted target of miR-769-5p in TargetScan and a prostate cancer recurrence-associated transcript (Fig. 4A). When all recurrence-associated transcripts in the dataset by Taylor *et al* (5) were plotted according to their corresponding hazard ratios, ARHGAP10 congregated with the gene group with hazard ratios ≤1, indicating its likely tumor suppressor role. Additional survival and correlation analyses were performed to test the relationship between miR-769-5p and ARHGAP10, expecting that if ARHGAP10 is truly a target of miR-769-5p, the two entities would be inversely correlated. The patients who had low expression of ARHGAP10 in their tumor had

Table I. Top 50 candidates from the RNAseq and TargetScan overlap for DU145 (n=322) and PC-3 (n=280).

Item	DU145	PC-3
RNAseq candidates (n)	623	592
TargetScan candidates (n)	3,661	3,661
Top 50 overlapping genes	SET, AGPAT1, MARCH8, RUNX3, CDKN2AIPNL, ATP6V1C1, RAB3D, B3GALT6, SSNA1, MEN1, GJB7, C17orf72, SLC45A3, CA13, UBE2D4, INHBE, KREMEN1, SH2D3C, CERCAM, LYRM9, COL5A1, SCAMP3, CCNDBP1, ARHGAP10, DDIT3, FAM167A, SLC35D1, HTR7, ASB13, FHL3, ABCG1, CPA4, CDH1, PHF5A, SYT3, TFAM, FAM117B, ZADH2, SPOCK1, TK2, KIF20A, MX2, WASF3, MSC, LRP12, HPCAL4, COPZ2, KCTD5, KIAA1199, LRP3	SET, RUNX3, CDKN2AIPNL, AGPAT1, MARCH8, COPZ2, ATP6V1C1, TFAM, CERCAM, NCCRP1, CDH1, BNC1, FBLN5, MEN1, FAM117B, LRP3, CCNDBP1, B3GALT6, SCAMP3, KREMEN1, XYLT1, SOD3, SSNA1, NUDT19, RAB3D, ZADH2, MX2, SERPINE1, SLC35D1, SNAI3, KIF20A, STRN4, PHF5A, REEP6, KCNE3, LRP12, ARHGAP10, KCTD5, EPSTI1, SLC44A4, WASF3, CPA4, VSIG10, RCC2, FOXO6, GPSM3, RSAD1, CHMP3, ASB13, TK2

RNAseq, RNA sequencing.

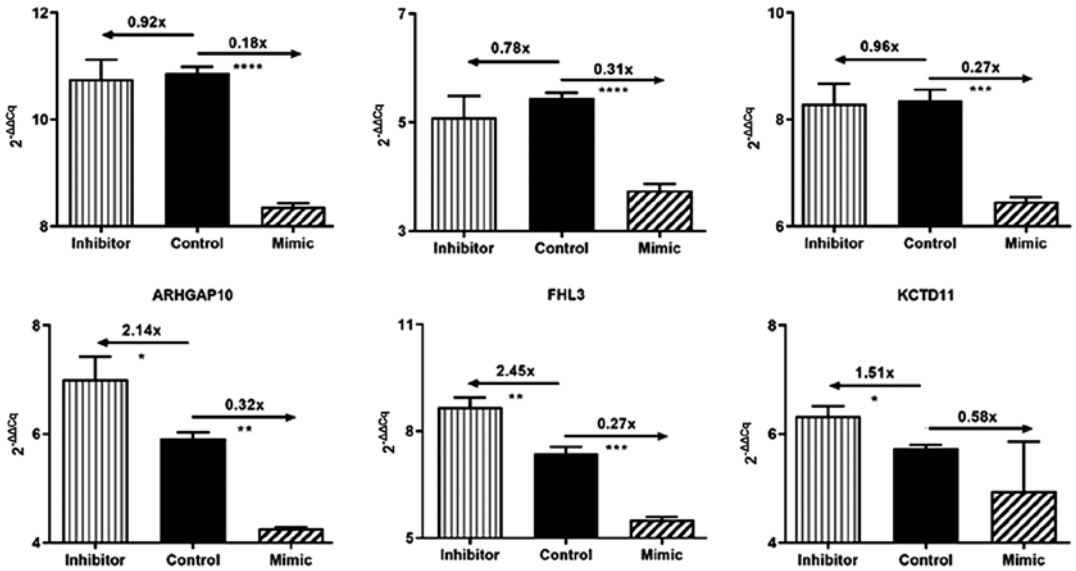

Gene	Log_2Fold Δ	p-value
AGPAT1	-2.342544364	3.27E-196
KREMEN1	-1.605017643	3.30E-64
CCNDBP1	-1.530549073	1.52E-108
ARHGAP10	-1.508622266	1.81E-59
FHL3	-1.463738119	1.02E-22
KCTD11	-1.271029508	7.73E-23

Figure 3. RT-qPCR analysis of predicted candidate targets of miR-769-5p. Top ranked candidate tumor suppressors were selected from the gene lists obtained from RNAseq data after transfection of DU145 and PC-3 cells with the miR-769-5p mimics. Their fold changes and P-values from RNAseq are listed in the embedded table. miR-769-5p inhibitor, negative control or miR-769-5p mimics were transfected into DU145 cells, followed by RT-qPCR to measure the expression of the predicted targets (n=3). Fold differences compared to the negative control miR group were calculated using the $2^{-\Delta\Delta Cq}$ method. *P<0.05, **P<0.01, ***P<0.001 and ****P<0.0001 according to Welch's ANOVA with Dunnett's test. AGPAT1, 1-acyl-sn-glycerol-3-phosphate acyltransferase α; KREMEN1, kremen protein 1; CCNDBP1, cyclin-D1-binding protein 1; ARHGAP10, Rho GTPase-activating protein 10; FHL3, four and a half LIM domains protein 3; KCTD11, potassium channel tetramerisation domain containing 11; miR, microRNA; RNAseq, RNA sequencing; RT-qPCR, reverse-transcription quantitative PCR.

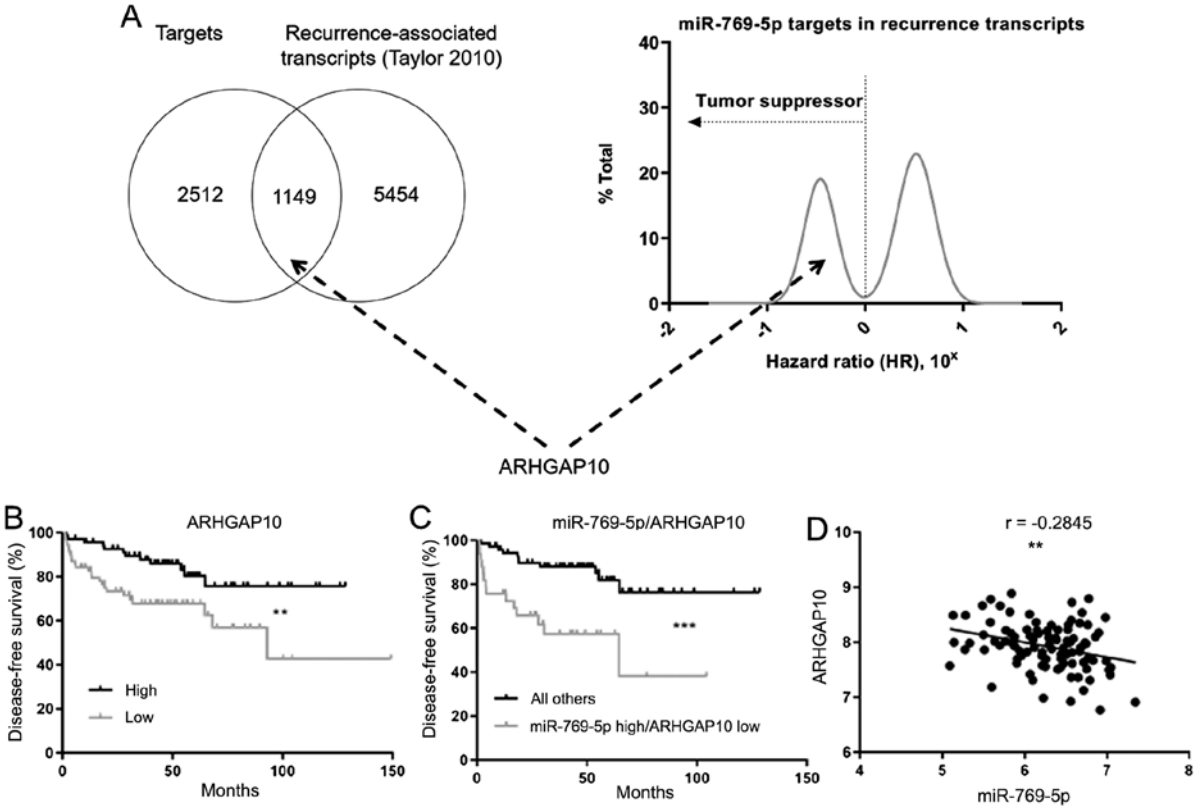

Figure 4. ARHGAP10 is a target of miR-769-5p and a tumor suppressor. (A) ARHGAP10 is at the intersection of the predicted targets of miR-769-5p and recurrence-associated transcripts (P<0.05 for continuous variables in the Cox proportional hazards regression). ARHGAP10 is a tumor suppressor using hazard ratio ≤1 as a criterion. Predicted targets are from TargetScan and recurrence-associated transcripts are from Taylor *et al* (5). (B) Patients with low expression of ARHGAP10 had reduced disease-free survival compared to those with high expression. (C) Patients with high expression of miR-769-5p and low expression of ARHGAP10 exhibited reduced disease-free survival compared to all others, **P<0.01, ***P<0.001 as per the log-rank test (n=140 in B and 105 in C. B- Low: 46 censored, 24 events. High: 58 censored, 12 events. C- miR-769-5p high/ARHGAP10 low: 19 censored, 14 events. All others: 61 censored, 11 events). (D) Inverse correlation between ARHGAP10 and miR-769-5p expression in prostate tumors (n=98) determined using Spearman correlation analysis; **P<0.01. Data were extracted from Taylor *et al* (5). ARHGAP10, Rho GTPase activating protein 10; miR, microRNA.

reduced survival (Fig. 4B), which further confirmed its role as a tumor suppressor in prostate cancer. Furthermore, patients who expressed miR-769-5p at a high level and ARHGAP10 at a low level in their tumor exhibited poor survival (Fig. 4C), consistent with a functional relationship that affects patient survival, and the two entities were also inversely correlated (Fig. 4D), providing additional evidence for this relationship.

miR-769-5p targets ARHGAP10 and influences cell survival. Based on the observations linking miR-769-5p and ARHGAP10, it was assessed whether miR-769-5p directly targets ARHGAP10. DU145 cells were transfected with luciferase reporter plasmids containing variations of the binding sequence from the 3'-UTR of ARHGAP10. The plasmids with the 3'-UTR sequences contained the WT or MUT binding sites for miR-769-5p and there were two predicted sites, which were mutated into MUT1, MUT2 or MUT1+2. miR-769-5p mimics significantly downregulated the luciferase activity of the plasmid containing the WT 3'-UTR, albeit moderately. By contrast, in the luciferase assays with the MUT1, MUT2 and MUT1+2 plasmids, the luciferase activity was not significantly affected by the miR-769-5p mimics (Fig. 5A), suggesting that both sites were binding targets of miR-769-5p.

When the cellular functions of miR-769-5p were assessed, it was noted that its inhibition consistently led to reduced proliferation of the 22Rv1, DU145 and PC-3 cell lines (Fig. 5B). Furthermore, it was assessed whether the reduced proliferation was a result of apoptosis by using caspase-3 as a readout. In 22Rv1 and PC-3 cells, caspase-3 increased significantly as a result of miR-769-5p inhibition (Fig. 5C). Therefore, miR-769-5p may have an oncogenic function to enhance the proliferation and inhibit apoptosis in at least a subset of human prostate cancer cell lines.

The anti-apoptotic effect of miR-769-5p is partially counteracted by ARHGAP10 through CDC42. Inhibition of miR-769-5p increased ARHGAP10 (Fig. 3) and ARHGAP10 was reported to bind CDC42 to inhibit its activity (10). Therefore, it was hypothesized that inhibition of miR-769-5p, leading to high ARHGAP10 levels, may reduce CDC42 activity in prostate cancer cells, which was experimentally confirmed (Fig. 6A). Furthermore, the combined inhibition of miR-769-5p and knockdown of ARHGAP10 negated the decreased CDC42 activity brought about by miR-769-5p inhibition alone. Accordingly, it was hypothesized that, similar to the relationship between ARHGAP10 and CDC42 in ovarian cancer (10), miR-769-5p, ARHGAP10 and CDC42 have a regulatory interaction in prostate cancer cells, i.e., miR-769-5p inhibits ARHGAP10, which suppresses CDC42. As a result of a reduction in ARHGAP10, CDC42 would then be

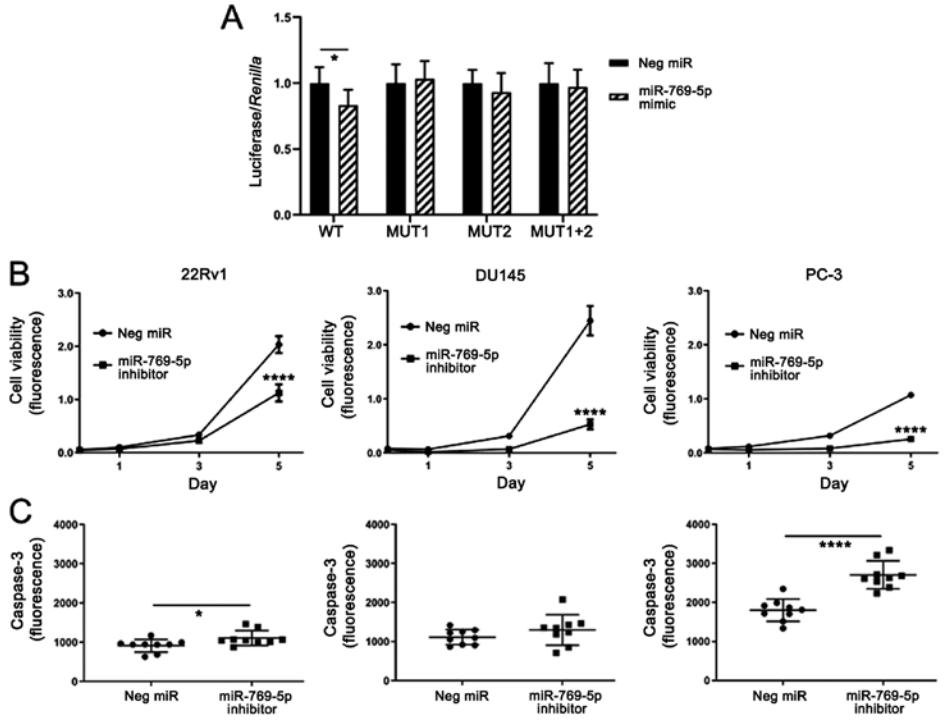

Figure 5. miR-769-5p targets ARHGAP10 and affects proliferation and apoptosis. (A) Sequence-verified WT 3'UTR, MUT1 3'UTR, MUT2 3'UTR or MUT1+2 3'UTR of ARHGAP10 was cloned into a luciferase reporter plasmid and transfected into DU145 human prostate cancer cells together with a *Renilla* plasmid for normalization and either negative control miR or miR-769-5p mimics. The Y-axis indicates the ratio of luciferase to *Renilla*, relative to the miRNA mimics, when the negative control was set at 1.0. (B) Reduced proliferation following inhibition of R-769-5p in three prostate cancer cell lines. (C) miR-769-5p inhibition significantly increases apoptosis in two human prostate cancer cell lines, as measured by caspase-3 activity, most noticeably in PC-3 cells. Values are expressed as the mean ± standard deviation (n=5 in A, 3 in B and 9 in C). *P<0.05, ****P<0.0001 according to unpaired t-test with Welch's correction. UTR, untranslated region; ARHGAP10, Rho GTPase activating protein 10; miR/miRNA, microRNA; MUT, mutant; WT, wild-type; Neg, negative control.

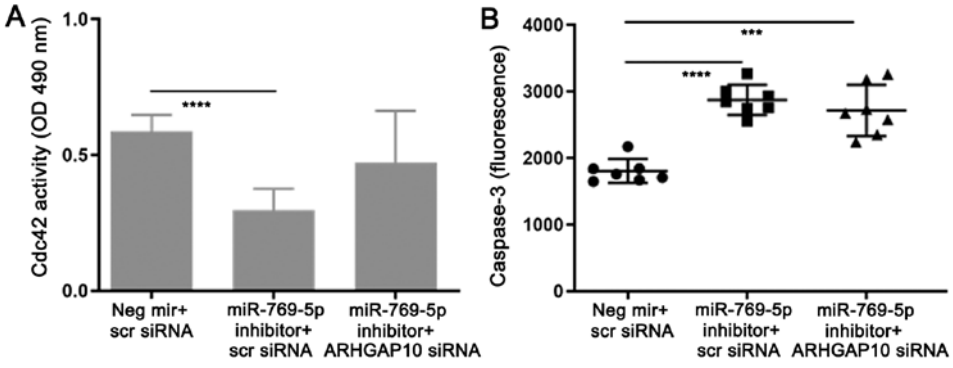

Figure 6. CDC42 activity and the effect of double transfection of miR-769-5p inhibitor and ARHGAP10 siRNA on apoptosis. (A) CDC42 activity was inversely associated with ARHGAP10, consistent with the literature; CDC42 activity was lower with miR-769-5p inhibitor vs. control miR. Combined miR-769-5p inhibition and ARHGAP10 knockdown increased CDC42 activity vs. miR-769-5p inhibition alone; thus, ARHGAP10 knockdown reversed the effect of miR-769-5p inhibition. (B) miR-769-5p inhibition increased apoptosis, which was slightly inhibited by ARHGAP10 knockdown (however, this effect was not remarkable). Values are expressed as the mean ± standard deviation (n=6 in A and 7 in B). ***P<0.001, ****P<0.0001 according to Welch's ANOVA with Dunnett's test. Scr, scrambled; CDC, cell division cycle; ARHGAP10, Rho GTPase activating protein 10; miR, microRNA; siRNA, small interfering RNA; OD, optical density; Neg, negative control.

upregulated. Next, it was assessed whether the combined inhibition of miR-769-5p and knockdown of ARHGAP10 reduces the increase in caspase-3 caused by miR-769-5p inhibition alone. The combined miR-769-5p inhibition and ARHGAP10 knockdown modestly reduced the increased caspase-3 activity caused by miR-769-5p inhibition alone (Fig. 6B). In other words, ARHGAP10 knockdown partially rescued the increased caspase-3 activity induced by inhibition of miR-769-5p.

Discussion

miRs have been reported to be involved in cancer. For instance, miR-155 targets von Hippel-Lindau for degradation and consequently upregulates angiogenesis in breast cancer (20). miR-19 degrades mitochondrial tumor suppressor 1 to increase proliferation and migration of lung cancer cells (21). Similarly, certain miRs are able to promote prostate carcinogenesis in numerous ways. miR-96 targets retinoid receptor γ (22),

which is reduced in prostate cancer, and miR-210-3p degrades TNFAIP3-interacting protein 1 and suppressor of cytokine signaling 1 (23), consequently activating NF-κβ signaling to increase migration, invasion and metastasis of prostate cancer cells. miR-27a-5p acts as a tumor suppressor in prostate cancer cells, where its inhibition promoted cell growth but its overexpression attenuated the malignant phenotype (24). Similarly, miR-197-3p functions as a tumor suppressor by reducing prostate cancer cell proliferation and colony formation, likely by downregulating phosphorylated Akt and β-catenin (25).

There have been various reports on the functions of miR-769-5p in the literature, which described its relevance in lung cancer. miR-769-5p was noted to be upregulated in hypoxic lung cancer cells and to affect their cell cycle by reducing the percentage of cells in S phase (26). Also in lung cancer, miR-769-5p was described to target transforming growth factor β receptor I to reduce proliferation, migration and invasion *in vitro* and tumor growth and metastasis *in vivo* (9). More studies are needed to elucidate the role of miR-769-5p in different malignancies, including prostate cancer. In the present study, it was indicated that miR-769-5p modulated the proliferation and apoptosis of prostate cancer cells. In contrast to the study on NSCLC (9), no significant relationship of miR-769-5p expression with cell migration or invasion was obtained in prostate cancer. Therefore, the functions of miR-769-5p are likely context- and organ-dependent.

The luciferase assays suggested that ARHGAP10 is targeted by miR-769-5p and the expression of the two entities was inversely correlated in human prostate tumors. These observations were noteworthy because ARHGAP10 has been previously reported to be a positive prognostic factor for overall survival in prostate cancer (11). In the present experiments, ARHGAP10 knockdown modestly reversed the caspase-3 increase brought about by miR-769-5p inhibition. This result implies that even though ARHGAP10 is involved in apoptosis of prostate cancer cells caused by miR-769-5p, additional mechanisms are likely involved. Therefore, gene targets of miR-769-5p in addition to ARHGAP10 may require to be knocked down before a full rescue is accomplished. Despite numerous attempts using different cell lines and reagents, western blots to detect ARHGAP10 were unsuccessful. No flow cytometry or western blot analysis was performed to confirm caspase-3 activation because EnzChek Caspase-3 Assay Kit #2 (Thermo Fisher Scientific, Inc. cat. no. E13184) is a reliable, sensitive and validated method consistent with western blot results (27-29). A limitation of the apoptosis experiments is that the cells were subjected to multiple transfections prior to the assay, which adds variability. Another limitation of the experiments in this study is that even though both DU145 and PC-3 are from metastases, DU145 worked better for migration than PC-3 with the xCELLigence system. In contrast, PC-3 worked better for invasion than DU145 with the system. Repetition of the motility experiments with additional cell lines would strengthen the findings.

In conclusion, miR-769-5p is a negative prognostic marker in prostate cancer, consistent with an oncogenic function to increase proliferation and inhibit apoptosis of prostate cancer cells. One of its binding targets evidenced through luciferase assay is ARHGAP10, whose knockdown partially reversed the effect of miR-769-5p inhibition on apoptosis. By highlighting the relevance of miR-769-5p and ARHGAP10 in prostate carcinogenesis, the present study shed light on future areas of research.

Acknowledgements

Not applicable.

Funding

This research was generously supported by the Medical Oncology Service and the Center for Cancer Research, National Cancer Institute, National Institutes of Health (Bethesda, USA).

Availability of data and materials

The datasets used and/or analyzed during the current study are available from the corresponding author on reasonable request.

Authors' contributions

DL performed the conception and design of the study, the experiments and bioinformatics analysis and writing of the manuscript. The author read and approved the final manuscript for publication.

Ethics approval and consent to participate

Not applicable.

Patient consent for publication

Not applicable.

Competing interests

The author declares that he has no competing interests.

References

1. Lee RC, Feinbaum RL and Ambros V: The *C. elegans* heterochronic gene lin-4 encodes small RNAs with antisense complementarity to lin-14. Cell 75: 843-854, 1993.
2. Hudson RS, Yi M, Esposito D, Watkins SK, Hurwitz AA, Yfantis HG, Lee DH, Borin JF, Naslund MJ, Alexander RB, *et al*: MicroRNA-1 is a candidate tumor suppressor and prognostic marker in human prostate cancer. Nucleic Acids Res 40: 3689-3703, 2012.
3. Hudson RS, Yi M, Esposito D, Glynn SA, Starks AM, Yang Y, Schetter AJ, Watkins SK, Hurwitz AA, Dorsey TH, *et al*: MicroRNA-106b-25 cluster expression is associated with early disease recurrence and targets caspase-7 and focal adhesion in human prostate cancer. Oncogene 32: 4139-4147, 2013.
4. Ambs S, Prueitt RL, Yi M, Hudson RS, Howe TM, Petrocca F, Wallace TA, Liu CG, Volinia S, Calin GA, *et al*: Genomic profiling of microRNA and messenger RNA reveals deregulated microRNA expression in prostate cancer. Cancer Res 68: 6162-6170, 2008.
5. Taylor BS, Schultz N, Hieronymus H, Gopalan A, Xiao Y, Carver BS, Arora VK, Kaushik P, Cerami E, Reva B, *et al*: Integrative genomic profiling of human prostate cancer. Cancer Cell 18: 11-22, 2010.
6. Schultz NA, Andersen KK, Roslind A, Willenbrock H, Wojdemann M and Johansen JS: Prognostic microRNAs in cancer tissue from patients operated for pancreatic cancer-five microRNAs in a prognostic index. World J Surg 36: 2699-2707, 2012.

7. Xie H, Lee L, Caramuta S, Höög A, Browaldh N, Björnhagen V, Larsson C and Lui WO: MicroRNA expression patterns related to merkel cell polyomavirus infection in human merkel cell carcinoma. J Invest Dermatol 134: 507-517, 2014.
8. Gasparini P, Cascione L, Landi L, Carasi S, Lovat F, Tibaldi C, Alì G, D'Incecco A, Minuti G, Chella A, *et al*: MicroRNA classifiers are powerful diagnostic/prognostic tools in ALK-, EGFR-, and KRAS-driven lung cancers. Proc Natl Acad Sci USA 112: 14924-14929, 2015.
9. Yang Z, He J, Gao P, Niu Y, Zhang J, Wang L, Liu M, Wei X, Liu C, Zhang C, *et al*: miR-769-5p suppressed cell proliferation, migration and invasion by targeting TGFBR1 in non-small cell lung carcinoma. Oncotarget 8: 113558-113570, 2017.
10. Luo N, Guo J, Chen L, Yang W, Qu X and Cheng Z: ARHGAP10, downregulated in ovarian cancer, suppresses tumorigenicity of ovarian cancer cells. Cell Death Dis 7: e2157, 2016.
11. Gong H, Chen X, Jin Y, Lu J, Cai Y, Wei O, Zhao J, Zhang W, Wen X, Wang Y and Chen W: Expression of ARHGAP10 correlates with prognosis of prostate cancer. Int J Clin Exp Pathol 12: 3839-3846, 2019.
12. Livak KJ and Schmittgen TD: Analysis of relative gene expression data using real-time quantitative PCR and the 2(-Delta Delta C(T)) method. Methods 25: 402-408, 2001.
13. Grasso CS, Wu YM, Robinson DR, Cao X, Dhanasekaran SM, Khan AP, Quist MJ, Jing X, Lonigro RJ, Brenner JC, *et al*: The mutational landscape of lethal castration-resistant prostate cancer. Nature 487: 239-243, 2012.
14. Lapointe J, Li C, Higgins JP, van de Rijn M, Bair E, Montgomery K, Ferrari M, Egevad L, Rayford W, Bergerheim U, *et al*: Gene expression profiling identifies clinically relevant subtypes of prostate cancer. Proc Natl Acad Sci USA 101: 811-816, 2004.
15. Singh D, Febbo PG, Ross K, Jackson DG, Manola J, Ladd C, Tamayo P, Renshaw AA, D'Amico AV, Richie JP, *et al*: Gene expression correlates of clinical prostate cancer behavior. Cancer Cell 1: 203-209, 2002.
16. Cancer Genome Atlas Research Network: The molecular taxonomy of primary prostate cancer. Cell 163: 1011-1025, 2015.
17. Tomlins SA, Mehra R, Rhodes DR, Cao X, Wang L, Dhanasekaran SM, Kalyana-Sundaram S, Wei JT, Rubin MA, Pienta KJ, *et al*: Integrative molecular concept modeling of prostate cancer progression. Nat Genet 39: 41-51, 2007.
18. Wallace TA, Prueitt RL, Yi M, Howe TM, Gillespie JW, Yfantis HG, Stephens RM, Caporaso NE, Loffredo CA and Ambs S: Tumor immunobiological differences in prostate cancer between African-American and European-American men. Cancer Res 68: 927-936, 2008.
19. Yu YP, Landsittel D, Jing L, Nelson J, Ren B, Liu L, McDonald C, Thomas R, Dhir R, Finkelstein S, *et al*: Gene expression alterations in prostate cancer predicting tumor aggression and preceding development of malignancy. J Clin Oncol 22: 2790-2799, 2004.
20. Kong W, He L, Richards EJ, Challa S, Xu CX, Permuth-Wey J, Lancaster JM, Coppola D, Sellers TA, Djeu JY and Cheng JQ: Upregulation of miRNA-155 promotes tumour angiogenesis by targeting VHL and is associated with poor prognosis and triple-negative breast cancer. Oncogene 33: 679-689, 2014.
21. Gu Y, Liu S, Zhang X, Chen G, Liang H, Yu M, Liao Z, Zhou Y, Zhang CY, Wang T, *et al*: Oncogenic miR-19a and miR-19b co-regulate tumor suppressor MTUS1 to promote cell proliferation and migration in lung cancer. Protein Cell 8: 455-466, 2017.
22. Long MD, Singh PK, Russell JR, Llimos G, Rosario S, Rizvi A, van den Berg PR, Kirk J, Sucheston-Campbell LE, Smiraglia DJ and Campbell MJ: The miR-96 and RARγ signaling axis governs androgen signaling and prostate cancer progression. Oncogene 38: 421-444, 2019.
23. Ren D, Yang Q, Dai Y, Guo W, Du H, Song L and Peng X: Oncogenic miR-210-3p promotes prostate cancer cell EMT and bone metastasis via NF-κB signaling pathway. Mol Cancer 16: 117, 2017.
24. Barros-Silva D, Costa-Pinheiro P, Duarte H, Sousa EJ, Evangelista AF, Graça I, Carneiro I, Martins AT, Oliveira J, Carvalho AL, *et al*: MicroRNA-27a-5p regulation by promoter methylation and MYC signaling in prostate carcinogenesis. Cell Death Dis 9: 167, 2018.
25. Huang Q, Ma B, Su Y, Chan K, Qu H, Huang J, Wang D, Qiu J, Liu H, Yang X and Wang Z: miR-197-3p represses the proliferation of prostate cancer by regulating the VDAC1/AKT/β-catenin signaling axis. Int J Biol Sci 16: 1417-1426, 2020.
26. Geng Y, Deng L, Su D, Xiao J, Ge D, Bao Y and Jing H: Identification of crucial microRNAs and genes in hypoxia-induced human lung adenocarcinoma cells. Onco Targets Ther 9: 4605-4616, 2016.
27. Chen S, Evans HG and Evans DR: FAM129B/MINERVA, a novel adherens junction-associated protein, suppresses apoptosis in HeLa cells. J Biol Chem 286: 10201-10209, 2011.
28. Detournay O and Weis VM: Role of the sphingosine rheostat in the regulation of cnidarian-dinoflagellate symbioses. Biol Bull 221: 261-269, 2011.
29. Hug H, Los M, Hirt W and Debatin KM: Rhodamine 110-linked amino acids and peptides as substrates to measure caspase activity upon apoptosis induction in intact cells. Biochemistry 38: 13906-13911, 1999.